Materials Research Proceedings 35 (2023) 232-240 https://doi.org/10.21741/9781644902714-28

Robust in-line qualification of lattice structures manufactured via laser powder bed fusion

Bianca Maria Colosimo[1,a], Marco Grasso[1,b *], Federica Garghetti[1,c] and Luca Pagani[2,d]

[1]Politecnico di Milano, Department of Mechanical Engineering, Via La Masa 1, 20156 Milano (Italy)

[2]GOM GmbH, Schmitztrasse 2, 38112 Braunschweig (Germany)

[a]biancamaria.colosimo@polimi.it, [b]marcoluigi.grasso@polimi.it, [c]federica.garghetti@polimi.it, [d]luca.paggy@gmail.com

Keywords: Additive Manufacturing, Quality Modelling, Profile Monitoring, Lattice, In-Situ Sensing

Abstract. The shape complexity enabled by AM would impose new part inspection systems (e.g., x-ray computed tomography), which translate into qualification time and costs that may be not affordable. However, the layerwise nature of the process potentially allows anticipating qualification tasks in-line and in-process, leading to a quick detection of defects since their onset stage. This opportunity is particularly attractive in the presence of lattice structures, whose industrial adoption has considerably increased thanks to AM. This paper presents a novel methodology to model the quality of lattice structures at unit cell level while the part is being built, using high resolutions images of the powder bed for in-line geometry reconstruction and identification of deviations from the nominal shape. The methodology is designed to translate complex 3D shapes into 1D deviation profiles that capture the "geometrical signature" of the cell together with the reconstruction uncertainty.

Introduction

Additive manufacturing (AM) technologies enable a variety of innovative product shapes, performances and functionalities that have been profitably exploited in a continuous increasing number of industrial applications. Among novel and most interesting geometries, lattice structures opened several opportunities in rethinking advanced and high-value-added components in sectors like healthcare, aerospace, space, and racing. Lattices are periodic structures made of unit cells of a predefined geometry that repeats in space, leading to enhanced performances thanks to a more efficient use of the material they are composed of [1]. Local inaccuracies may have a detrimental effect on the functional performance of the whole structure [2 – 4]. As an example, a local dimensional and/or geometrical mismatch between the manufactured part and the nominal geometry may influence the mechanical properties together with the type of failure mechanism [2]. However, there is still a lack of statistical methods to model and monitor the quality of these structures in industry.

A seminal approach proposed in [5] was aimed to transform the 3D deviation between the ex-situ reconstructed geometry of the lattice (via X-ray computed tomography (CT)) and its nominal geometry into 1D deviation profiles that captured a layerwise deviation metric on a cell-by-cell basis. Colosimo et al. [5] showed that the proposed approach enabled the detection of local geometrical distortions in one cell or in one sub-portion of the lattice. An even higher potential for industrial adoption of such lattice structure modelling and monitoring methodology would involve the possibility to move from ex-situ (post-process) to in-situ (in-process) measurements, taking advantage of layerwise image data collection in AM. Exploiting in-situ and in-line data would

Materials Research Proceedings 35 (2023) 232-240 https://doi.org/10.21741/9781644902714-28

allow end-users to anticipate the detection of anomalies and defects while the part is being produced, enabling possible remedy actions (e.g., part suppression), reducing both post-process inspection costs and material wastes. In-line geometry reconstruction and monitoring could be also combined with advanced process control and first-time-right strategies, to heal and mitigate deviations from the nominal shape (see for example [6 – 8]). Colosimo et al. [9] introduced an extension of the aforementioned method that replaces ex-situ X-ray CT measurements with in-situ powder bed images. The authors devoted special attention to the challenges imposed by various sources of variability that may affect the in-situ geometry reconstruction. The authors proposed a methodology that combines a robust active contour algorithm for solidified layer image segmentation with a robust fitting technique to enhance the reconstruction accuracy. Another approach was proposed by Guerra et al. [10], where authors used powder bed images to generate a 3D optical tomography reconstruction of the printed structure for dimensional and geometrical characterization. The authors showed the potential use of the method to detect process inaccuracies and geometric distortions.

The present study inherits the robust reconstruction and modelling approach presented in [9], and it extends that work with two additional and novel analyses. The first regards the quantitative evaluation of the reconstructions accuracy that can be achieved via in-situ active contour segmentation of a lattice structure. The second involves the performance analysis of a robust fitting approach applied to 1D deviation profiles, in terms of deviation from the nominal shape. The aim is to demonstrate to what extent in-situ deviation models could be effective in replacing more complex and expensive ex-situ gathered ones.

Differently from Guerra et al. [10], the lattice geometry was reconstructed by means of high-resolution powder bed images rather than using a long-exposure optical tomography image. The proposed in-situ robust active contour segmentation was compared against the CT-based reconstruction used as a reference (or ground truth) to highlight the agreement of dimensional measurements obtained with the two different data sources. As far as the cell-wise 1D deviation profile reconstruction is concerned, a quantitative analysis of the benefits provided by the proposed robust model compared with a traditional least square fitting is presented too. Robust modelling represents a key issue to reduce the uncertainty of deviation estimates for the design of statistical process monitoring tools that may leverage on the proposed in-situ modelling and qualification framework.

A lattice structure production using an industrial laser powder bed fusion (L-PBF) system is presented as real case study. The original camera and lighting setup available as embedded off-the-shelf equipment was used, which allows evaluating the suitability of the proposed approach for implementation on an industrial L-PBF platform with no need for machine modification.

The paper is organized as follows. Section 2 presents the case study. Section 3 briefly describes the methodology, and Section 4 presents the major results. Section 5 concludes the paper.

Case Study

As a real case study, a maraging steel lattice structure produced via L-PBF on an industrial Trumpf TruPrint 3000 system was considered. The structure was composed by 64 equal rhombic cells, with a nominal struct thickness equal to 1.5 mm. The overall specimen dimension was 40 × 40 × 40 mm, with a nominal cubic cell envelope with side equal to 10 mm. The specimen was produced with two lateral walls of thickness equal to 0.6 mm, removed from the analysis of the current work. A gas atomized powder was used and nominal process parameters provided by the machine vendor were applied. Fig. 1 shows the manufactured part, the nominal geometry of the rhombic cell and the process parameters used for the experiment.

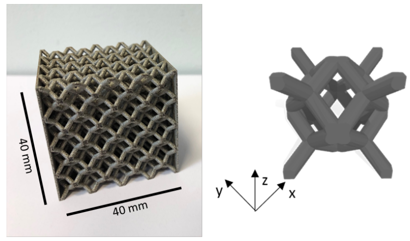

Scan strategy	Meandering
Scan mode	Continuous mode
Laser power	275 W
Laser speed	1200 mm/s
Hatch distance	0.09 mm
Layer thickness	0.05 mm

Fig. 1 Printed part, nominal unit cell and process parameters (the meandering scan direction was rotated by 67° every layer)

The Trumpf TruPrint 3000 machine has an integrated powder bed camera (Basler acA3800-14uc USB 3.0 camera) that allows capturing post-deposition and post-melting images with an instant field of view (spatial resolution) of 100 μm/pixel. The light source was inclined of about 60° with respect to the building plate. It consists of a LED stripe on the ceiling of the chamber.

The specimen was inspected using a North Star Imaging X25 x-ray CT scan system with a voxel size of 33 μm. The 3D shape reconstructed ex-situ was first aligned with respect to the nominal geometry (via Iterative Closest Point (ICP) registration) and then sliced with a slice thickness equal to the layer thickness used during the L-PBF process. This allowed the superimposition of both the in-situ and ex-situ geometry reconstructions in every layer for comparison purpose. The surface determination was performed via the proprietary algorithm "standard classic" implemented in VGStudio Max. The uncertainty of the geometry reconstructed via x-ray CT is mainly affected by the i) surface determination error and ii) the ICP registration error. Minimizing these errors allows enhancing the suitability of the x-ray CT as ground truth. In this study, algorithms implemented in VGStudio Max were used as representative of the current industrial practice. Nevertheless, other state-of-the-art methods can be considered to further enhance the ground truth accuracy [11 - 12]. Generally speaking, x-ray CT represents the current state of the art for the reconstruction of the actual shape, as it is commonly used for product acceptance, and its uncertainty is one order of magnitude lower than the one of in-situ reconstructions with standard powder bed cameras, which makes x-ray CT suitable as a ground truth.

Methodology

Before applying the proposed approach, a pre-processing of powder bed images is need to perform a perspective correction and to align the resulting images against the nominal geometry. Standard algorithms may be used to this aim, see for example [13 – 14]. The methodology then consists of three steps: i) segmentation of each solidified layer, ii) estimation of a deviation metric to quantify the deviation between the in-situ reconstructed shape and the nominal one in each layer, iii) robust modelling of the deviation as a function of the build direction for each single unit cell.

Regarding image segmentation, we advocate the active contour methodology [15 – 16]. In entails an iterative segmentation procedure that starts from a first boundary definition in the form of a closed curve and adapts it by applying shrink/expansion operations until the boundary converges to the final reconstructed contour. In L-PBF, the nominal geometry itself can be used as starting boundary [17 – 19]. A robust variant of the active contour method was shown in [19] to be particularly effective in powder bed image segmentation. It combines edge-based and region-based active contours segmentation operations:

$$\frac{\delta\varphi(x,t)}{\delta t} = w(t)\delta_{region} + (1 - w(t))\delta_{edge} \tag{1}$$

where $\varphi(x)$ is the signed distance function in pixel location x, which is iteratively varied until convergence to the final reconstructed contour; δ_{region} is the region-based term, δ_{edge} is the edge-based term, and $w(t)$ such that $0 \leq w(t) \leq 1$ is a weight to balance the influence of each term.

As proposed in [19], the weight $w(t)$ may vary as a function of the iteration counter, t, associating higher weight to the region-based term in initial iterations, for rough contour adjustments, and higher weight to the edge-based term in last iterations, for a final fine-tuning of the contour. The reader is referred to [19] for full details. The active contour algorithm can be calibrated and tuned using a reference geometry and its x-ray CT reconstruction as a ground truth. Calibration is envisaged to take into account the specific conditions imposed by the L-PBF machine and its machine vision and illumination setup.

The underlying idea is that by combining region- and edge-based segmentations, a more robust reconstruction of the actual contour is achieved, in a way that is robust to pixel intensity variations within foreground and background areas. The output of the segmentation consists of a binary image, where background pixels have intensity $I = 0$, and foreground pixels (solidified layer) have intensity $I = 1$. Since both the in-situ reconstructed shape and its nominal geometry are represented in binary format, the deviation between them can be computed as:

$$\delta_{i,j,k}(z) = \frac{1}{N}\sum_l \mathcal{I}(I_{insitu}(l) - I_{nominal}(l) \neq 0)_{i,j,k}, \text{ for the } (i,j,k)^{th} \text{ cell} \quad (2)$$

where z is the build direction, N is the number of pixels within the analyzed region of the powder bed image, $\mathcal{I}(\cdot)$ is the indicator function, $I_{insitu}(l)$ is the value the l^{th} pixel of the binarized powder bed image generated by the active contours segmentation, and $I_{nominal}(l)$ is the value of the l^{th} pixel of the binary image representing the nominal shape. Each unit cell is identified by the indexes (i,j,k), which refers to the location of the cell along the X, Y and Z directions, respectively, inside the lattice structure.

The aim of the proposed approach consists of modelling the $\delta_{i,j,k}(z)$ at unit cell-level. In [5], a B-spline basis defined as:

$$C_{i,j,k}(z) = \sum_{q=1}^{Q+L-1} B_q(z,\tau)P_{i,j,k,q} \quad (3)$$

where B_q are the B-Spline basis functions of order $Q = 3$, $\boldsymbol{\tau} = \{\tau_l, l = 1,2,\ldots,L-1\}$ is the B-spline knot sequence, L is the number of subintervals, and $P_{i,j,k,1}, P_{i,j,k,2}, \ldots, P_{i,j,k,Q+L-1}$ are the control points for the $(i,j,k)^{th}$ unit cell. The standard B-spline model is fitted via the least squares (LS) method, and it implies that all levels z, namely all layers, are equally trustworthy. However, when the deviation profile must be estimated from powder bed images, a layerwise variation of pixel intensity patterns may lead to a layerwise variation of the reconstructed contour accuracy. Some layers may exhibit a so-called *bright field* condition, because the solidified layer produces intense light reflections towards the camera: a high intensity of foreground pixels is known to yield poor edge detection results, as they tend to force the segmentation algorithms to isolate the brightest area rather than the whole foreground region. Other layers may exhibit a so-called *dark field* condition, where most of light is reflected in other directions. This condition is known to be the most appropriate for accurate edge detection. Switching from one condition to the other, being fixed the chamber lighting setup, occurs as a consequence of the layerwise varying scan direction. We thus propose a robust approach to give a higher weight to layer where a dark-field pattern is present and lower weight to the ones where a bright-field is present. The final goal is to gather a more accurate prediction $\hat{\delta}_{i,j,k}(z)$ of the 1D deviation from the nominal shape, relying more on layers where more accurate geometry reconstruction is expected.

Since a bright-field condition yields a higher pixel intensity within the foreground, we propose a weighting scheme where the weight $\omega_{i,j,k}(z)$ is proportional to the inverse of the variance $s_{i,j,k}(z)^2$ of pixel intensities within a region of interest Ω such that:

$$\omega_{i,j,k}(z) = \frac{1}{S}\frac{1}{s_{i,j,k}(z)^2} \quad (4)$$

where $S = \sum_k \frac{1}{s_{i,j,k}(k)^2}$ is just a corrective factor. The region of interest Ω can be either the bounding box of the part within the build area, including both the solidified layer and the surrounding powder, or a reduced region that adapts, layer by layer, to the geometry of the part. We advocate this latter approach. Colosimo et al. [9] proposed a method to define such region as an envelope (or a band) that is centred on the contour of the nominal geometry in the layer, and extend by one half within the foreground, and by the other half within the background (loose powder). The same approach was used here to define such region (full details are referred to [9] for sake of space). Since background pixel intensities in one location are assumed to be quite stable from one layer to another, the underlying rationale is the following: a high value of $s_{i,j,k}(z)^2$ within the region of interest adaptively identified in each layer implies a higher intensity of foreground pixels compared to background ones, which is common in bright field conditions. The opposite is expected in the presence of a dark field, where foreground and background pixels are expected to have more similar intensities. Thus, low values of $\omega_{i,j,k}(z)$ penalize layers where a poor reconstruction accuracy is expected because of the bright field. B-spline control points can be computed using the weighted least squares (WLS) method:

$$P_{i,j,k} = \left(B^T W_{i,j,k}(z) B\right)^{-1} B^T W_{i,j,k}(z) \delta_{i,j,k}(z) \quad (5)$$

where B is the model matrix and $W_{i,j,k}(z)$ is a diagonal matrix whose diagonal elements are the weights $\omega_{i,j,k}(z)$. In this study, a simple knot sequence $\boldsymbol{\tau}$ composed by 21 equi-spaced knots was used, but the knot sequence may be tailored in principle depending on the specific geometry of the lattice cell. It is worth noticing that: i) due to illumination inhomogeneity, different parts in the same build area may exhibit different bright or dark field conditions, and hence wights can be computed on a part-by-part basis rather than on a layer-by-layer basis, ii) bright and dark field conditions are highly dependent on the scan direction, and hence the a-priori knowledge about the scan direction in each layer may be used to enhance the weighting procedure.

Results

Fig. 2 shows two examples of powder bed images in two different layers, where the raw image was superimposed to three contours, namely the ex-situ reconstruction obtained via X-ray CT, the nominal contour, and the in-situ reconstruction generated by the proposed robust active contour methodology. Fig. 2 shows that the in-situ reconstruction is in good agreement with the other two reference contours.

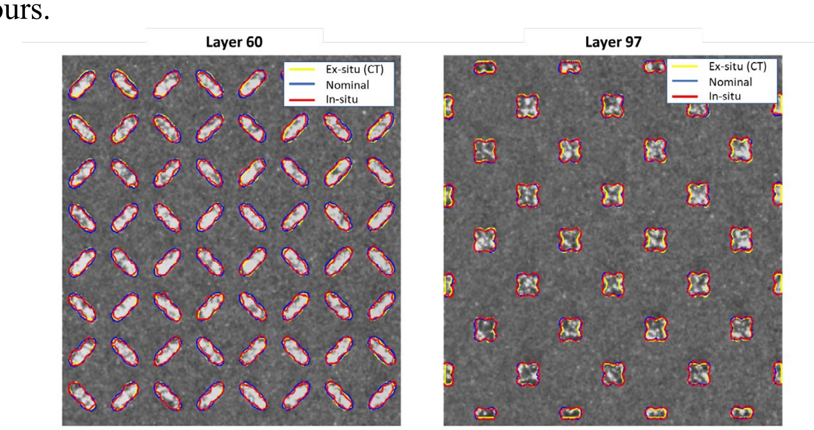

Fig. 2 – Example of two layers with in-situ and ex-situ reconstructions compared to the nominal one

To quantitatively determine the accuracy of the in-situ reconstruction with respect to the one achieved via ex-situ CT, Eq. 2 was used by replacing the nominal shape with the CT reference. The powder bed images were clustered into two sets by applying a K-means clustering with K = 2 to the values of weights $\omega_{i,j,k}(z)$. The result was a separation of layers with lower weights (corresponding to bright field conditions) from layers with higher weights (corresponding to dark field conditions). For each set, a 95% confidence interval (CI) of the mean deviation between the in-situ and ex-situ geometry reconstructions were computed. Fig. 3 shows two examples of powder bed images belonging to the two clusters, and the 95% CIs of the mean deviations.

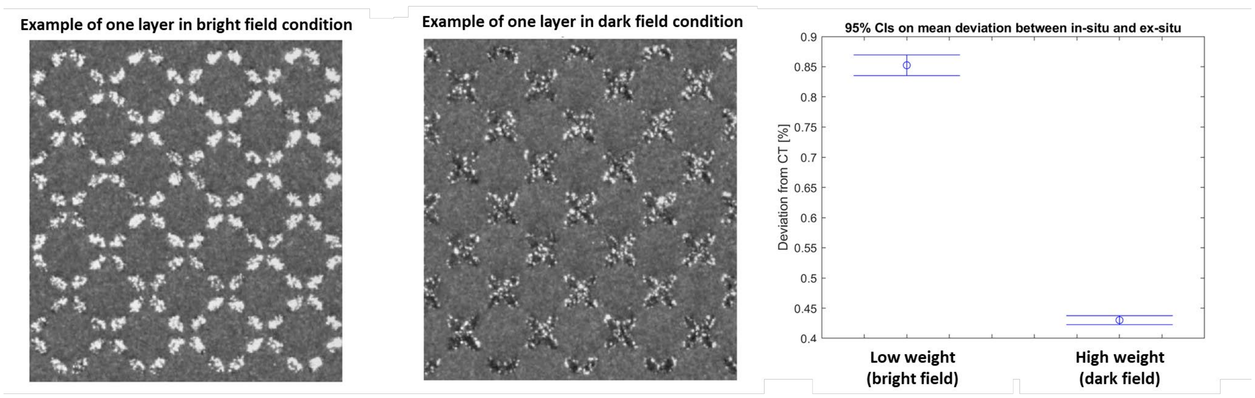

Fig. 3 – Two examples of layers characterized by a bright field and a dark field pattern (right) and 95% CIs on the mean deviation between in-situ and ex-situ reconstructed shapes in these two different conditions

Fig. 3 (right panel) shows that when a dark field pattern is present, the in-situ reconstruction is significantly closer to the CT-reconstructed shape used as a ground truth than in the presence of a bright field condition. Fig. 3 (right panel) also shows that the proposed weighting scheme is effective in separating layers characterized by a poor reconstruction from those characterize by a good one. Finally, the mean deviation between in-situ and ex-situ reconstructed shapes under dark field conditions is quite small (average lower than 0.45%), much less than in bright field conditions (average of about 0.85%). In terms of strut thickness it corresponds to an average deviation between 0.05 and 0.1 mm.

The proposed approach is not simply aimed to yield a good layerwise reconstruction of the part, but also to generate a synthetic representation of the deviation from the nominal geometry that is suitable to capture the salient "signature" of each unit cell while allowing a data format that is easier and more efficient to handle than the full 3D shape. To this aim, the WLS fitting approach was tested on the deviation profiles of all 64 unit cells. Fig. 4 (left panels) shows the WLS fitting and the model residuals for all the unit cells. The proposed WLS model filters out the effect of bright field patterns on the resulting 1D fitted deviation profile, enhancing the whole deviation pattern estimate. In order to quantify the benefits of the proposed WLS approach, a comparison against a traditional LS model based on the same B-spline basis (but without any weighting scheme applied to individual layers) is shown in Fig. 4, right panel. The comparison involves two performance metrics, namely the root mean square (RMS) of the predicted deviation from the nominal, and the variance of the prediction (95% bootstrap confidence intervals are shown).

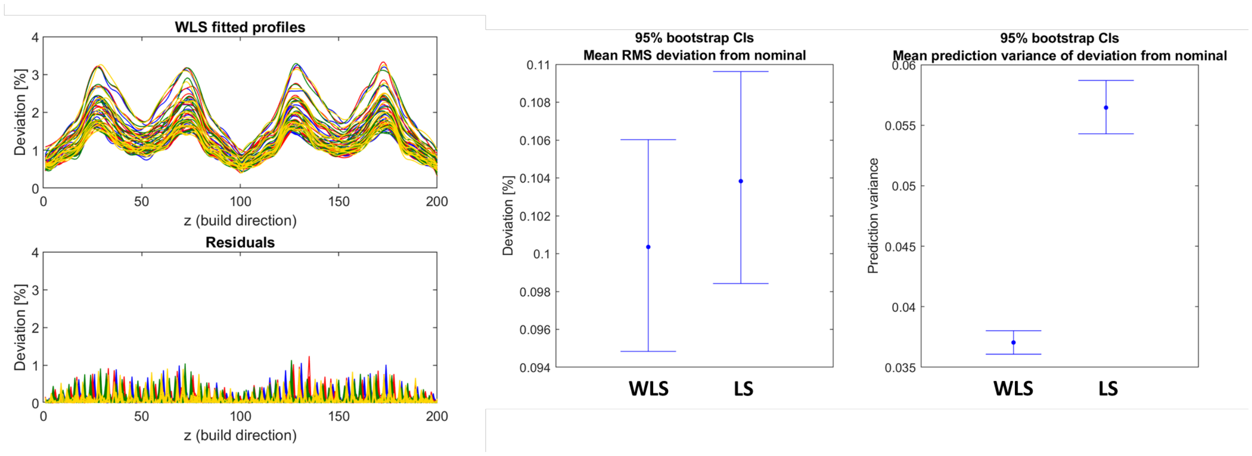

Fig. 4 – Left: WLS fitted deviation profiles and residuals; right: 95% bootstrap CIs for the mean RMS deviation from the nominal and the mean prediction variance of deviation from the nominal for WLS and LS models

Fig. 4 (right panels) shows that, in terms of RMS, the two models are not statistically different, but the WLS model yields a much lower prediction variance, i.e., a more precise estimate of the geometry deviation signature. This latter result is highly relevant for the design of statistical process monitoring methods that may take advantage of in-situ deviation profiles, as a lower associated variance implies a higher power in detecting out-of-control deviations caused by anomalous distortions. It is worth noticing that the pattern of the fitted profiles is highly influenced by the actual shape of the cell, with peaks in correspondence of lattice nodes and a symmetry along Z that inherits the unit cell symmetry. Thus, the deviation profile can be regarded as a signature of the specific lattice geometry.

Conclusions

The increased shape complexity of high-value-added products enabled by AM technologies has opened a variety of new challenges concerning efficient product qualification methodologies and statistical quality monitoring instruments. Post-process ex-situ CT inspections, despite their actual effectiveness, are often too expensive and time-consuming to meet high productivity constraints. In this study, we presented a method to support the in-line qualification of complex shapes like lattice structures, which can be used to anticipate the detection of geometrical distortions and to possibly reduce the need for post-process inspections. A key issue is the accuracy of in-situ geometry reconstructions and estimates, as powder bed images are affected by variability sources that are not present in X-ray CT. The analysis presented in this study highlighted that in presence of favourable pixel intensity patterns, the accuracy of in-situ lattice reconstruction is very close to the one obtained via ex-situ measurements. Moreover, by reconstructing the cell-wise 1D deviation profile with the proposed weighted fitting method, it is possible to filter out nuisance effects caused by layers exhibiting lower reconstruction accuracy, finally leading to a more accurate and precise estimation of the lattice geometrical signature.

An on-going work will extend this analysis to multiple lattice components, exploring different deviation metrics as well as one novel way to take into explicit account the spatial dependence of deviation profiles in unit cells of the same structure and/or of different structures in the same build. The performance analysis of the proposed approach in the presence of actual geometrical distortions is under development too. The authors are working on other promising research directions, including novel solutions to augment the sensing setup to further improve the accuracy of in-situ quality estimates and possible extensions of the proposed framework to more complex geometries and different families of lattice structure. Another development regards the study of spatial correlation among profiles associated to different unit cells, which may further enhance the characterization of the natural variability as well as the defect detection performance.

References

[1] Helou, M., & Kara, S. (2018). Design, analysis and manufacturing of lattice structures: an overview. International Journal of Computer Integrated Manufacturing, 31(3), 243-261. https://doi.org/10.1080/0951192X.2017.1407456

[2] Liu, L., Kamm, P., García-Moreno, F., Banhart, J., & Pasini, D. (2017). Elastic and failure response of imperfect three-dimensional metallic lattices: the role of geometric defects induced by Selective Laser Melting. Journal of the Mechanics and Physics of Solids, 107, 160-184. https://doi.org/10.1016/j.jmps.2017.07.003

[3] Melancon, D., Bagheri, Z. S., Johnston, R. B., Liu, L., Tanzer, M., & Pasini, D. (2017). Mechanical characterization of structurally porous biomaterials built via additive manufacturing: experiments, predictive models, and design maps for load-bearing bone replacement implants. Acta biomaterialia, 63, 350-368. https://doi.org/10.1016/j.actbio.2017.09.013

[4] Dallago, M., Raghavendra, S., Luchin, V., Zappini, G., Pasini, D., & Benedetti, M. (2019). Geometric assessment of lattice materials built via Selective Laser Melting. Materials Today: Proceedings, 7, 353-361. https://doi.org/10.1016/j.matpr.2018.11.096

[5] Colosimo B.M., Grasso, M., Garghetti, F., Rossi, B. (2021), Complex geometries in additive manufacturing: A new solution for lattice structure modeling and monitoring, Journal of Quality Technology. https://doi.org/10.1080/00224065.2021.1926377

[6] Liu, C., Le Roux, L., Ji, Z., Kerfriden, P., Lacan, F., & Bigot, S. (2020). Machine Learning-enabled feedback loops for metal powder bed fusion additive manufacturing. Procedia Computer Science, 176, 2586-2595. https://doi.org/10.1016/j.procs.2020.09.314

[7] Vasileska, E., Demir, A. G., Colosimo, B. M., & Previtali, B. (2020). Layer-wise control of selective laser melting by means of inline melt pool area measurements. Journal of Laser Applications, 32(2), 022057. https://doi.org/10.2351/7.0000108

[8] Colosimo, B. M., Grossi, E., Caltanissetta, F., & Grasso, M. (2020). Penelope: a novel prototype for in situ defect removal in LPBF. Jom, 72, 1332-1339. https://doi.org/10.1007/s11837-019-03964-0

[9] Colosimo, B. M., Garghetti, F., Pagani, L., & Grasso, M. (2022). A novel method for in-process inspection of lattice structures via in-situ layerwise imaging. Manufacturing Letters, 32, 67-72. https://doi.org/10.1016/j.mfglet.2022.03.004

[10] Guerra, M. G., Lafirenza, M., Errico, V., & Angelastro, A. (2023). In-process dimensional and geometrical characterization of laser-powder bed fusion lattice structures through high-resolution optical tomography. Optics & Laser Technology, 162, 109252. https://doi.org/10.1016/j.optlastec.2023.109252

[11] Dewulf, W., Bosse, H., Carmignato, S., & Leach, R. (2022). Advances in the metrological traceability and performance of X-ray computed tomography. CIRP Annals, 71(2), 693-716. https://doi.org/10.1016/j.cirp.2022.05.001

[12] Withers, P. J., Bouman, C., Carmignato, S., Cnudde, V., Grimaldi, D., Hagen, C. K., ... & Stock, S. R. (2021). X-ray computed tomography. Nature Reviews Methods Primers, 1(1), 18. https://doi.org/10.1038/s43586-021-00015-4

[13] Szeliski, R. (2022). Image alignment and stitching. In Computer Vision (pp. 401-441). Springer, Cham. https://doi.org/10.1007/978-3-030-34372-9_8

[14] Avants, B.B., Tustison, N.J., Stauffer, M., Song, G., Wu, B., Gee, J.C. (2014) The insight toolkit image registration framework, Front. Neuroinform. 8(44). https://doi.org/10.3389/fninf.2014.00044

[15] Liu, S., & Peng, Y. (2012). A local region-based Chan-Vese model for image segmentation. Pattern Recognition, 45(7), 2769-2779. https://doi.org/10.1016/j.patcog.2011.11.019

[16] Soomro, S., Munir, A., & Choi, K. N. (2018). Hybrid two-stage active contour method with region and edge information for intensity inhomogeneous image segmentation. PloS one, 13(1), e0191827. https://doi.org/10.1371/journal.pone.0191827

[17] Caltanissetta, F., Grasso, M., Petro, S., & Colosimo, B. M. (2018). Characterization of in-situ measurements based on layerwise imaging in laser powder bed fusion. Additive Manufacturing, 24, 183-199. https://doi.org/10.1016/j.addma.2018.09.017

[18] Aminzadeh, M., & Kurfess, T. (2016, June). Vision-based inspection system for dimensional accuracy in powder-bed additive manufacturing. In International manufacturing science and engineering conference (Vol. 49903, p. V002T04A042). American Society of Mechanical Engineers. https://doi.org/10.1115/MSEC2016-8674

[19] Pagani, L., Grasso, M., Scott, P. J., & Colosimo, B. M. (2020). Automated layerwise detection of geometrical distortions in laser powder bed fusion. Additive Manufacturing, 36, 101435. https://doi.org/10.1016/j.addma.2020.101435